Commensurate-incommensurate supersolid ground state of a spin-orbit-coupled Bose-Einstein condensate in one-dimensional optical lattices

Shuai Li,[1,2] Huan Wang,[1,2] Fuli Li,[1,2] Xiaoling Cui,[3,4] and Bo Liu[1,2,*]

[1]*Department of Applied Physics, School of Physics, Xi'an Jiaotong University, Xi'an 710049, Shaanxi, China*

[2]*Shaanxi Province Key Laboratory of Quantum Information and Quantum Optoelectronic Devices, Xi'an Jiaotong University, Xi'an 710049, Shaanxi, China*

[3]*Beijing National Laboratory for Condensed Matter Physics, Institute of Physics, Chinese Academy of Sciences, Beijing, 100190, China*

[4]*Songshan Lake Materials Laboratory, Dongguan, Guangdong 523808, China*

(Received 29 September 2019; revised 16 July 2020; accepted 10 August 2020; published 18 September 2020)

Recent experimental advances to create tunable synthetic spin-orbit coupling (SOC) in ultracold gases provide new possibilities to access fruitful spin-orbit coupled quantum many-body physics. In this paper, we demonstrate that the combined effect of two-dimensional (2D) SOC and one-dimensional (1D) optical lattice in interacting bosons can provide an alternative scheme in ultracold gases to achieve the crossover of the commensurate-incommensurate supersolid ground state "with respect to the background optical lattice." Interestingly, it is shown that the anharmonicity arising from the lattice potential leads to the "pin" effect and make the ground-state break the continuous translational symmetry along the direction perpendicular to the 1D lattice, whereas the competition between the lattice period and the SOC length results in the crossover of commensurate-incommensurate ground state along the direction of 1D lattice with discrete translational symmetry breaking. Such a combined effect of SOC and optical lattice, thus, induces a new 2D periodic pattern in the ground state, accompanying with nonzero 2D superfluid density characterizing the supersolid nature in 2D of the ground state. Furthermore, a skyrmion-anti-skyrmion lattice is found associated with the appearance of such supersolid ground state, indicating its topological nontrivial properties. Experimental signature of our proposed supersolid ground state is also predicted by means of the time-of-flight measurement.

DOI: 10.1103/PhysRevA.102.033328

I. INTRODUCTION

The supersolid, a fascinating quantum state of matter, is characterized by two independent spontaneously broken symmetries, i.e., $U(1)$ and translational symmetries with corresponding superfluidity and density order [1,2]. Such a long-sought quantum state of matter shows a variety of novel properties, such as the nonclassical rotational inertia and other anomalous transport features [3–6]. It, thus, has attracted tremendous interests in both theoretical and experimental studies in solids and atomic matter systems. For example, a supersolid was predicted to exist in bulk helium, but to prove its existence is still an open question in recent experiments [7–15]. Thanks to the high controllability in ultracold atomic gases, there have been great interests in searching such supersolids via ultracold atoms in both experimental and theoretical studies. It was previously predicted to appear in polar molecules, magnetic, and Rydberg atoms [16–21]. There have recently been some exciting experimental progresses in exploring supersolid properties of Bose-Einstein condensates (BECs) of highly magnetic atoms [22–24]. Besides that, a stripe phase with supersolid properties has also been observed in spin-orbit-coupled BECs, which links the SOC with supersolidity [25,26]. Recent experimental realization of synthetic SOC in cold atomic gases [27–31] possesses highly tunable parameters, such as the form and strength of the SOC, and system geometry tuned by the confined potential. Such flexible control greatly extends the horizon of quantum simulation of supersolidity in cold atomic gases.

Here, we report the emergence of the crossover of commensurate-incommensurate supersolid ground state, induced by the combined effect of two-dimensional (2D) SOC and one-dimensional (1D) optical lattice in interacting bosons. The key idea, here, is to utilize the effect of mixed dimensionality engineered from the combination of the confined potential and SOC. Interestingly, it is shown that in a 2D spin-orbit coupled interacting boson gas, the anisotropic confinement resulting from the 1D lattice potential leads to the "pin" effect and the ground state, thus, breaks the continuous translational symmetry perpendicular to the tightly confined spatial dimension along the 1D lattice. On the other hand, along the direction of the 1D lattice, the competition between the lattice period and the SOC length results in the crossover of the commensurate-incommensurate ground state with discrete translational symmetry breaking. Such a combined mixed-dimensionality effect of the 2D SOC and the 1D optical lattice, thus, induces a new 2D periodic pattern in the ground state, accompanying with the nonzero 2D superfluid density characterizing its supersolid nature. Furthermore, such a supersolid ground state also possesses an exotic topological spin texture where a skyrmion-anti-skyrmion lattice is formed associated with the appearance of supersoildity.

*liubophy@gmail.com

II. TWO-DIMENSIONAL SUPERSOLID GROUND STATE

Let us consider a trapped quasi-two-dimensional spin-1/2 interacting Bose gas in the presence of both a Rashba-type SOC and a one-dimensional optical lattice. Such a system can be described by the following model Hamiltonian:

$$\hat{H} = \int d^2\mathbf{r}\,\Psi^\dagger\left[\frac{\mathbf{k}^2}{2m} + V_{\text{trap}}(\mathbf{r}) + V_{\text{OL}}(\mathbf{r}) + \frac{\kappa}{m}\mathbf{k}\cdot\hat{\sigma}\right]\Psi + \int d^2\mathbf{r}(g_1\hat{n}_\uparrow^2 + g_2\hat{n}_\downarrow^2 + 2g_{12}\hat{n}_\uparrow\hat{n}_\downarrow), \tag{1}$$

where $V_{\text{OL}}(\mathbf{r}) = V_0\sin^2(k_L x)$ is a 1D optical lattice along the x direction. V_0 is the lattice depth, and k_L is the wave vector of the laser field with the corresponding lattice constant defined as $a_L = \pi/k_L$. $\Psi = (\Psi_\uparrow, \Psi_\downarrow)^T$ labels the Bose field operators for two pseudospin bosons. κ describes the strength of the Rashba-type SOC, and $\hat{\sigma}$ is the Pauli matrix. The density operators for two pseudospin bosons are defined as $\hat{n}_\uparrow = \Psi_\uparrow^\dagger\Psi_\uparrow$, $\hat{n}_\downarrow = \Psi_\downarrow^\dagger\Psi_\downarrow$, respectively. g_1 and g_2 characterize the intraspecies contact interaction strength, whereas g_{12} labels the interspecies contact interaction strength. Those are determined by the effective intraspecies and interspecies s-wave scattering length, respectively. In this paper, we will focus on the case with $g_1 = g_2 > 0$. $V_{\text{trap}}(\mathbf{r}) = \frac{1}{2}m\omega^2(x^2+y^2)$ is an isotropic harmonic trap mimicking the practical situation in cold atom experiments. Here, we choose $\hbar\omega$, $\sqrt{\hbar/m\omega}$, and $1/\omega$ as the units of energy, spatial length, and time, respectively. Then, the ground state can be found numerically by minimizing the following dimensionless energy functional constructed under the Gross-Pitaevskii mean-field theory,

$$\varepsilon = \int d^2\mathbf{r}\sum_{\sigma=\uparrow,\downarrow}\psi_\sigma^*\left[-\frac{1}{2}\nabla^2 + \frac{1}{2}(x^2+y^2) + V_0'\sin^2(k_L' x)\right]\psi_\sigma + \kappa'[\psi_\uparrow^*(-i\partial_x - \partial_y)\psi_\downarrow + \psi_\downarrow^*(-i\partial_x + \partial_y)\psi_\uparrow] + \frac{c_0'}{2}(|\psi_\uparrow|^2 + |\psi_\downarrow|^2)^2 + \frac{c_2'}{2}(|\psi_\downarrow|^2 - |\psi_\uparrow|^2)^2, \tag{2}$$

where $V_0' = V_0/\hbar\omega$ is the dimensionless lattice depth and the dimensionless wave vector is defined as $k_L' = k_L\sqrt{\hbar/m\omega}$. The dimensionless interaction strength is defined as $c_0' = \beta_1 + \beta_{12}$ and $c_2' = \beta_1 - \beta_{12}$, where $\beta_1 = g_1 Nm/\hbar^2$ and $\beta_{12} = g_{12}Nm/\hbar^2$ with the total particle number N. And the dimensionless SOC strength is $\kappa' = \kappa/\sqrt{\hbar m\omega}$.

Through numerically computing the ground state via minimizing the dimensionless energy functional in Eq. (2) by using the imaginary time-evolution method, the phase diagram is obtained as shown in Fig. 1(a). Note that the phase diagram, here, is constructed in the weakly interacting regime where the kinetic energy is much larger than both intraspecies and interspecies interaction energies. It is confirmed in our numerics that the interaction energy is typically smaller than the kinetic energy by two orders of magnitude. Therefore, in such a region, the Gross-Pitaevskii mean-field theory is valid. As shown in Fig. 1(a), there are two different regions in the phase diagram, which consists of a superfluid stripe and a supersolid ground state. A threshold of lattice depth separates the above two different regions when considering a fixed Rashba SOC strength. Below that lattice depth threshold, the ground state of the system is a superfluid stripe. Whereas further increasing the lattice depth above the critical value, a supersolid ground state will be favored.

Here, we would like to stress the significant effect of mixed dimensionality engineered from the combination of lattice potential and SOC to explain the appearance of our proposed supersolid ground state. When increasing the lattice depth, the 1D optical lattice in the two-dimensional system can be considered as an array of tubes, and each one of them is elongated along the direction perpendicular to the 1D lattice. Such highly anisotropic confinement leads to the pin effect in a 2D spin-orbit coupled interacting boson gas (see details in the Appendix) and a periodic density modulation along the vertical direction as shown in Fig. 1(b) is spontaneously formed in the ground state and, thus, breaks the continuous translational symmetry. On the other hand, along the direction of the 1D lattice, the combined effect of SOC and lattice potential not only causes a periodic density modulation coincided with the lattice period as shown in Fig. 1(b), but also introduces an additional phase modulation of the ground-state wave function. For instance, as shown in Fig. 1(c), there is an additional π-phase modulation in the ground-state wave function along the direction of the 1D lattice because the interplay of SOC and the lattice potential leads bosons to condensate at $\pm\frac{\pi}{a_L}$ in that direction. Therefore, such a ground state breaks the discrete translational symmetry of the background lattice. The combined mixed-dimensionality effect of the 2D SOC and the 1D optical lattice, thus, induces a new symmetry-breaking ground state in 2D, i.e., continuous and discrete translational symmetry breaking along the vertical and horizontal directions, respectively. Combined with the $U(1)$ gauge symmetry breaking, such a ground state can, thus, be considered as a supersolid state. To further capture the superfluid property of our proposed supersolid ground state as shown in the inset of Fig. 1(a), there is a finite superfluid density (see the details in the Appendix), implying the existence of off-diagonal long-range order. The nonzero SOC will suppress the superfluid density, which may be understood from the softening of the low-energy excitation modes [32,33]. The transition between the superfluid and the supersolid is characterized by a discontinuous jump in the superfluid density as shown in the inset of Fig. 1(a), that reflects its first-order nature.

More interestingly, the significant effect resulting from the interplay of the SOC and the lattice characteristic lengths is also unveiled in our scheme. As shown in Fig. 1(a), there are two regions of the supersolid ground state. When the strength of SOC is large enough, i.e., the SOC length is much smaller than the optical lattice period a_L, we find that the

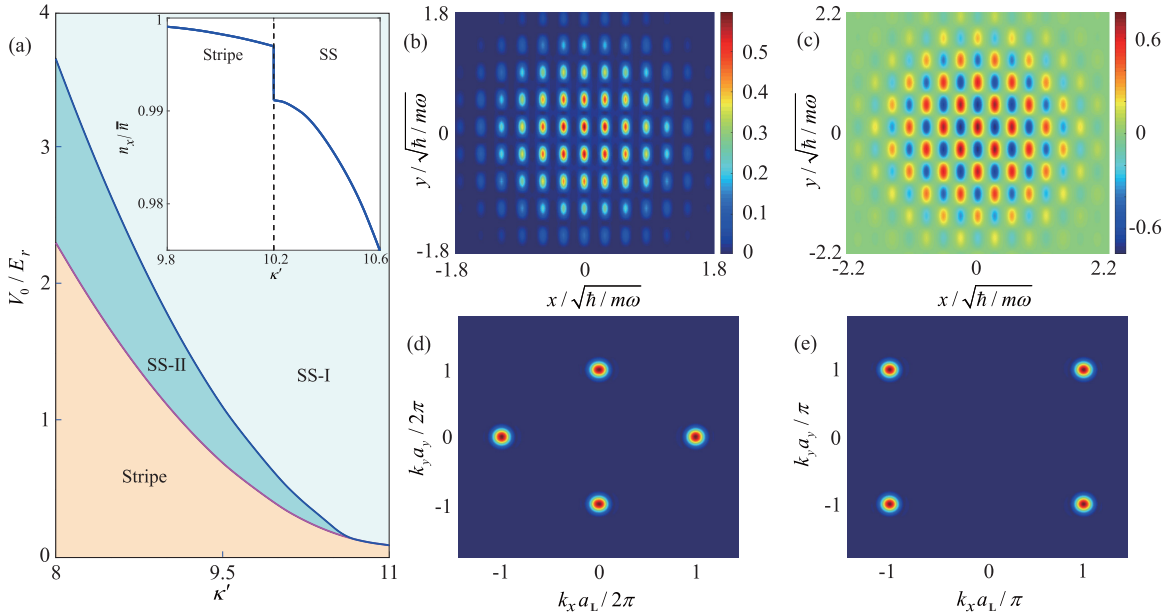

FIG. 1. (a) Zero-temperature phase diagram of the model Hamiltonian in Eq. (1) as a function of the SOC strength κ' and lattice depth V_0/E_r. E_r is the recoil energy. For certain SOC, there is a threshold of the lattice depth, beyond that the supersolid ground state appears. There are two regions of the supersolid ground state. SS-I stands for the region where the period of the supersolid ground-state wave function along the horizontal direction is fixed by $2a_L$. Whereas in SS-II, the supersolid ground-state wave function has a continuously changed period along the horizontal direction. The inset shows that there is a jump in the superfluid density (see details in the Appendix) when the transition from the superfluid to the supersolid ground state occurs. Panels (b) and (d) show the density profile of the supersolid ground state for the spin-up component. In (b), it is shown that a spatially periodic rectangle density distribution is formed. The periodicity of such a density profile is determined by the period of lattice potential and SOC for the horizontal and vertical directions, respectively. In (d), the corresponding momentum density distribution with respect to (b) is shown. To demonstrate the periodic structure, in (d), we just show the oscillatory portion of the density distribution by eliminating the effect of the background average density profile. Panels (c) and (e) show the supersolid ground-state wave function (real part) for the spin-up component. There is an additional π-phase modulation in the ground-state wave function along the direction of the 1D lattice because of the existence of finite-momentum BECs and the period of ground-state wave function along the horizontal direction is $2a_L$. Therefore, such a ground state breaks the discrete translational symmetry of the background lattice. In (e), the corresponding wave function in momentum space with respect to (c) is shown. In (b)–(e), we choose $V_0/E_r = 2.98$, $\kappa' = 10.8$, whereas in the inset of (a), $V_0/E_r = 0.17$. Other parameters are chosen as $c_0' = 10$, $c_2' = -0.8c_0'$, and $k_L' = 3.5\pi$. a_y is the spatial periodicity of the density distribution along the y direction.

length scale of the optical lattice takes the dominant effect on the system and the period of the ground-state wave function along the horizontal direction is, thus, fixed by $2a_L$. Whereas decreasing the strength of SOC, being comparable to the lattice period, the competition between the optical lattice period and the SOC length plays an important role and surprisingly makes the ground-state wave function have a continuously changed period along the horizontal direction. As shown in Fig. 2 for the fixed lattice depth, the period of the ground-state wave function along the horizontal direction becomes a continuous function of the strength of SOC, leading to a smooth crossover between the commensurate and the incommensurate supersolid ground state. Through numerics, we confirm that the ground-state energy is a continuous function when changing the strength of SOC, indicating its crossover nature rather than a transition. Furthermore, a characteristic feature of the wave function in momentum space can be used to distinguish a supersolid ground state. Specifically, as shown in Fig. 1(e), there are peaks of the ground-state wave function in momentum space located at $(\pm\frac{\pi}{a_L}, \pm\frac{\pi}{a_y})$, indicating the periodic structure of our proposed supersolid ground state in 2D. Here, a_y is the spatial periodicity of density distribution along the y direction. Such a characteristic feature of the supersolid ground-state wave function, i.e., peaks in momentum space, can be detected using conventional time-of-flight imaging technique, for instance, as shown in Fig. 3 where the expansion image after a time t is given by $\tilde{n}_\sigma(\mathbf{x}) = (m/\hbar t)^2 G_\sigma(\tilde{\mathbf{k}})$ with $\tilde{\mathbf{k}} = m\mathbf{x}/\hbar t$, $G_\sigma(\tilde{\mathbf{k}}) = \int e^{i\tilde{\mathbf{k}}\cdot(\mathbf{r}-\mathbf{r}')}\psi_\sigma^*(\mathbf{r})\psi_\sigma(\mathbf{r}')d^2\mathbf{r}\,d^2\mathbf{r}'$, and atom mass m.

The supersolid ground state proposed here also exhibits exotic spin textures, which will be discussed below. To demonstrate that, let us first define a spin density vector for the spin-1/2 bosons as $\mathbf{S} = \mathbf{\Psi}^\dagger \boldsymbol{\sigma} \mathbf{\Psi}/|\mathbf{\Psi}|^2$ with $\boldsymbol{\sigma}$ representing the Pauli matrix. As shown in Fig. 4(a), the spin texture represents a periodic magnetic structure accompanying with the emergence of the supersolid. If we zoom in on such a spin texture, there are two different structures. As shown in Figs. 4(b) and 4(c), the vector $\mathbf{S}$ wraps around a sphere, and it points to the south (north) pole in the center, whereas with increasing radius, it varies continuously and eventually points to the north (south) pole. Therefore, the vector $\mathbf{S}$ forms skyrmions (antiskyrmions). It is also shown that the skyrmion and

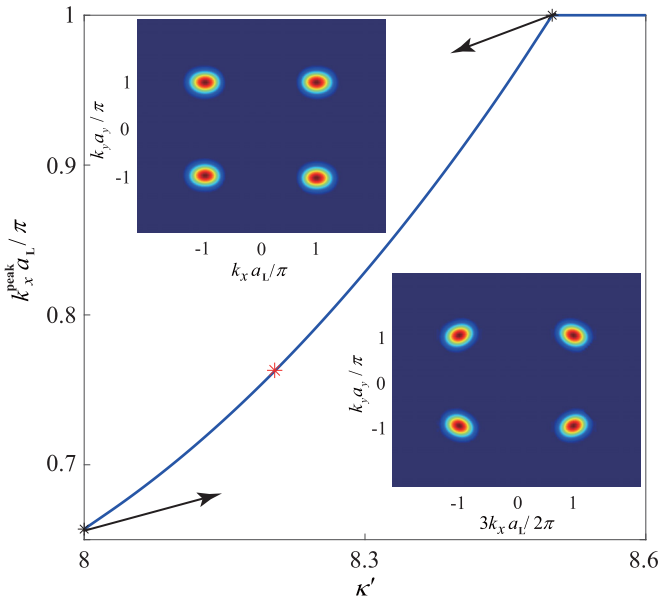

FIG. 2. The period of the supersolid ground-state wave function along the horizontal direction as a function of the strength of SOC with certain lattice depth. Here, $k_x^{\rm peak}$ labels the positive condensate momentum along the horizontal direction. It is shown that such period behaves as a continuous function of the strength of SOC, leading to a smooth crossover between the commensurate and the incommensurate supersolid ground states. The insets show the commensurate supersolid ground-state wave function (real part) in the momentum space with the horizontal periods $2a_L$ and $3a_L$, respectively. The incommensurate supersolid ground state is shown, for example, by the red mark with horizontal period $6/\sqrt{5}a_L$. The other parameters are chosen as $c_0' = 10,\ c_2' = -0.8c_0',\ k_L' = 3.5\pi$, and $V_0/E_r = 2.65$.

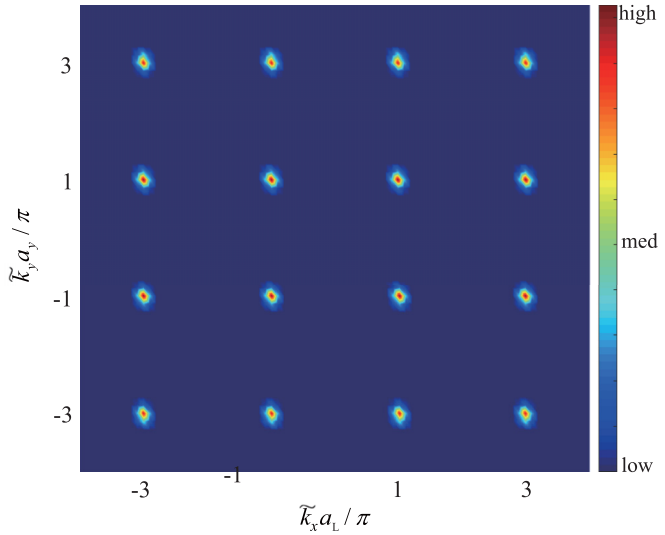

FIG. 3. The expansion image of the supersolid ground state for the spin-up component. It is shown that the location of peaks coincide with the results as shown in Figs. 1(c) and 1(e). The appearance of larger periodicity with respect to the lattice period in the x direction is indicative of the broken discrete translational symmetry of the background lattice. The other parameters are the same as in Fig. 1(c).

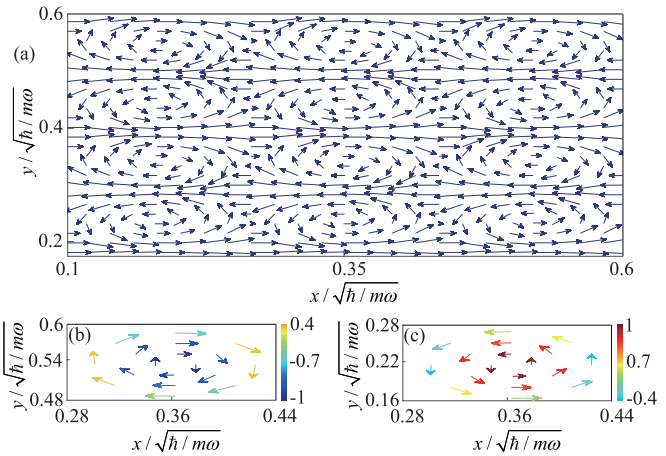

FIG. 4. The skyrmion-anti-skyrmion lattice spin texture of the proposed supersolid ground state. (a) Illustration of the skyrmion-anti-skyrmion lattice configuration formed by the vector S defined in the main text. It is shown that the x and y components of S form a vortex-anti-vortex lattice structure on the xy plane. (b) and (c) show the skyrmion and antiskyrmion, respectively. Here, the arrows show (S_x, S_y) and the colors index the z component of S. Other parameters are chosen as $c_0' = 20,\ c_2' = -0.8c_0',\ k_L' = 8\pi,\ \kappa' = 30,\ V_0' = 7$.

antiskyrmion spin textures appear at where the spin-down and spin-up components are centralized, respectively. The cores of the spin structure as shown in Fig. 4(a) are correspondingly centered around the minimum of density distributions for spin-up and spin-down components along the horizontal direction. Such spin textures are, thus, formed by a skyrmion-anti-skyrmion lattice coinciding with the appearance of the supersolid. Our scheme, hence, provides an alternative way to create and manipulate exotic spin textures in spin-orbit coupled ultracold gases. The topological nature of the above spin structures can be characterized by the topological charge Q, which can be defined as a spatial integral of the topological charge density,

$$Q = \int d^2\mathbf{r} \frac{1}{4\pi} \mathbf{S} \cdot \left(\frac{\partial \mathbf{S}}{\partial x} \times \frac{\partial \mathbf{S}}{\partial y} \right). \tag{3}$$

Since the $\mathcal{P}T$ symmetry, associated with the operations $\mathcal{T} = i\sigma_y \mathcal{C}$ with $\mathcal{C}$ taking the complex conjugate and $\mathcal{P} = \sigma_z \mathcal{I}$ with spatial inversion operator $\mathcal{I}$, is broken in our proposed supersolid ground state, its topologically nontrivial property can be captured by a Z_2 topological invariance. Therefore, the associated topological invariants do not depend on the superfluid fraction. It is confirmed from our numerics where we find that a skyrmion carries a topological charge 1, whereas an antiskyrmion carries a topological charge -1, distinguished from the topologically trivial case where the topological charge is zero.

III. CONCLUSION

To summarize, we have demonstrated an alternative approach to achieve 2D supersolidity via the combined effects of the 2D SOC and the 1D optical lattice in interacting bosons. The significant effect resulting from the competition between the optical lattice period and the spin-orbit coupling length is

unveiled, which leads to the crossover of the commensurate-incommensurate supersolid ground state. Our proposed supersolid ground state also possesses a nontrivial topological property, characterized by an associated exotic spin texture, i.e., a skyrmion-anti-skyrmion spin lattice. Our approach is rather generic to the spin-orbit coupled quantum gases than restricted to the setup considered in this paper. Its principle is readily generalizable to the spin-orbit coupled systems with higher spin.

ACKNOWLEDGMENTS

This work was supported by the National Key Research and Development Program of China (Grants No. 2018YFA0307600, No. 2016YFA0300603, and No. 2016YFA0301404) and NSFC Grants No. 11774282, No. 11622436, No. 11421092, No. 11534014, and No. 11534008. B.L. acknowledges the Cyrus Tang Foundation Young Scholar Program and the Fundamental Research Funds for the Central Universities. We also thank the HPC platform of Xi'An Jiaotong University where our numerical calculations were performed.

APPENDIX A: ANHARMONICITY INDUCED PIN EFFECT

In this Appendix, we will provide a detailed description of the pin effect resulting from the anisotropic confinement induced by the 1D lattice in a 2D spin-orbit coupled interacting boson gas. Let us consider a trapped quasi-two-dimensional spin-1/2 interacting Bose gas in the presence of a Rashba-type SOC. It can be described by the following model Hamiltonian $\hat{H} = \hat{H}_0 + \hat{H}_{\rm int}$, where

$$\hat{H}_0 = \int d^2\mathbf{r}\, \Psi^\dagger \left[\frac{\mathbf{k}^2}{2m} + V_{\rm trap}(\mathbf{r}) + \frac{\kappa}{m}\mathbf{k}\cdot\hat{\sigma}\right]\Psi \tag{A1}$$

is the single-particle Hamiltonian with $\Psi = (\Psi_\uparrow, \Psi_\downarrow)^T$ denoting the Bose field operators for two pseudospin bosons. The Rashba-type SOC is captured by the last term in $\hat{H}_0$ with κ describing the strength of SOC, and $\hat{\sigma}$ being the Pauli matrix. The interaction part of $\hat{H}$ can be expressed as

$$\hat{H}_{\rm int} = \int d^2\mathbf{r}(g_1\hat{n}_\uparrow^2 + g_2\hat{n}_\downarrow^2 + 2g_{12}\hat{n}_\uparrow\hat{n}_\downarrow). \tag{A2}$$

In this paper, we will focus on the case with $g_1 = g_2 > 0$. When further considering the presence of an isotropic harmonic trap $V_{\rm trap}(\mathbf{r}) = \frac{1}{2}m\omega^2(x^2+y^2)$ mimicking the practical situation in cold atom experiments, it is known that the ground state is a superfluid stripe phase in the region where $c_2/c_0 < 0$ with $c_0 = g_1 + g_{12}$ and $c_2 = g_1 - g_{12}$. Due to the spatially isotropic property of the harmonic trap, the stripe phase along different directions is energetically degenerate where the direction of the stripe phase is determined by the condensate momentum. To break this spatially rotational symmetry, one can consider utilizing the anisotropy of the trapping potential. Interestingly, we find that the anharmonic trap, i.e., anisotropic confinement, will pin the direction of density stripe.

To demonstrate this, let us consider compressing the isotropic harmonic trap into a cigar shape, and the corresponding trapping potential can be written as $V_{\rm Atrap}(\mathbf{r}) = \frac{1}{2}m\omega^2(\gamma x^2 + y^2)$ with γ describing the anisotropy. When $\gamma > 1$, the trapping potential becomes elliptical with the long axis residing in the y direction (vertical direction), and the short axis along the x direction. Without loss of generality, we further set the long axis of the elliptical trapping potential located at a certain angle θ_0 with respect to the y axis. Then, the ground state can be found numerically by minimizing the following dimensionless energy functional constructed under the Gross-Pitaevskii mean-field theory,

$$\begin{aligned}\varepsilon = \int d^2\mathbf{r} \sum_{\sigma=\uparrow,\downarrow} \psi_\sigma^* \left[-\frac{1}{2}\nabla^2 + V_{{\rm Atrap},\theta_0}(\mathbf{r})\right]\psi_\sigma \\ + \kappa'[\psi_\uparrow^*(-i\partial_x - \partial_y)\psi_\downarrow + \psi_\downarrow^*(-i\partial_x + \partial_y)\psi_\uparrow] + \frac{c_0'}{2}(|\psi_\uparrow|^2 \\ + |\psi_\downarrow|^2)^2 + \frac{c_2'}{2}(|\psi_\downarrow|^2 - |\psi_\uparrow|^2)^2.\end{aligned} \tag{A3}$$

Here, we choose $\hbar\omega$, $\sqrt{\hbar/m\omega}$, and $1/\omega$ as the units of energy, spatial length, and time, respectively. $V_{{\rm Atrap},\theta_0}(\mathbf{r}) = \frac{1}{2}[\gamma(\cos\theta_0 x + \sin\theta_0 y)^2 + (\cos\theta_0 y - \sin\theta_0 x)^2]$ represents the anharmonic trap with the long axis located at the angle θ_0 with respect to the vertical direction. The dimensionless interaction strength is defined as $c_0' = \beta_1 + \beta_{12}$ and $c_2' = \beta_1 - \beta_{12}$, where $\beta_1 = g_1 Nm/\hbar^2$ and $\beta_{12} = g_{12}Nm/\hbar^2$ with the total particle number N. And the dimensionless SOC strength is $\kappa' = \kappa/\sqrt{\hbar m\omega}$. What we found is shown in Fig. 5. For example, in the presence of an anharmonic trap with

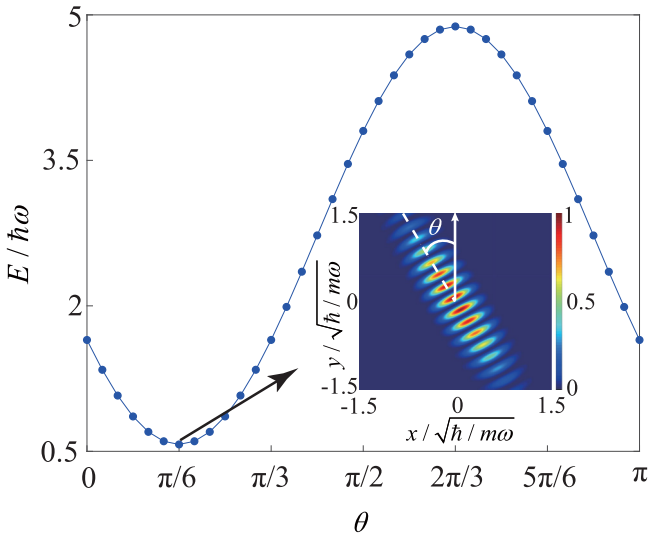

FIG. 5. The expectation value of the energy E contributed from the anharmonic trap $V_{{\rm Atrap},\theta_0}(\mathbf{r})$ for different superfluid stripe phases pointing along the direction located at angle θ with respect to the vertical direction. Here, we choose the long axis of the anharmonic trap located at angle $\theta_0 = \pi/6$. It is shown that the stripe phase pointing along the long axis of the trapping potential mostly minimizes the energy cost compared to all the other direction-pointing stripe phases. The inset shows the stripe phase pointing along $\theta = \pi/6$ where the dashed line indicates the direction determined by the polar angle of the condensate momentum. The polar axis, here, is set as the positive y axis. Other parameters are chosen as $\gamma = 15$, $\kappa' = 14$, $c_0' = 2$, and $c_2' = -0.8c_0'$.

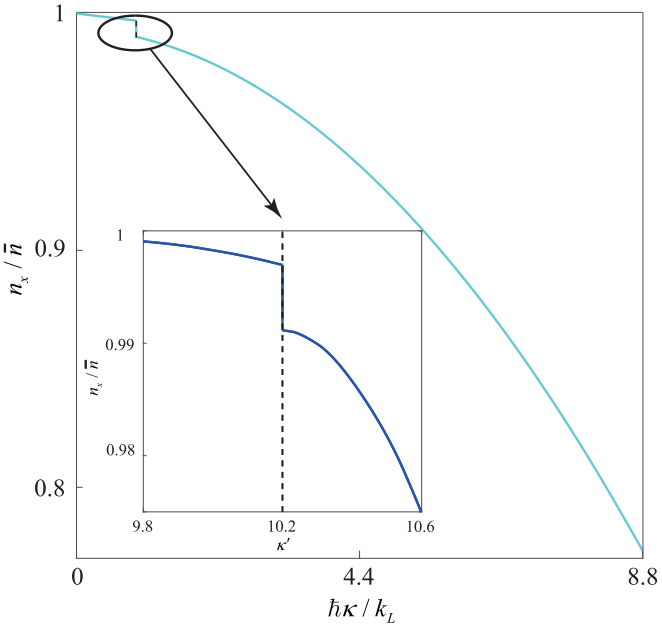

FIG. 6. Superfluid density n_x as the function of strength of SOC. There is a jump in the superfluid density when the transition from the superfluid to the supersolid occurs. The other parameters are chosen as $c_0' = 10,\ c_2' = -0.8c_0',\ k_L' = 3.5\pi$, and $V_0/E_r = 0.17$.

the long axis located at the angle $\theta_0 = \pi/6$, the stripe phase pointing the long axis of the trap mostly minimizes the energy resulting from the trapping potential compared to all the other direction-pointing stripe phases. Since the kinetic energy and interaction energy are the same for the stripe phases pointing along different directions, the anharmonic trap will pin the direction of the stripe phase along the long axis of the trap where the system will be energetically favored.

When the lattice depth is deep enough, the 1D optical lattice in the two-dimensional system can be considered as an array of tubes. Each one of them is elongated along the direction perpendicular to the 1D lattice. Such highly anisotropic confinement, thus, leads to the pin effect as described above and a periodic structure along the vertical direction is formed in the ground state.

APPENDIX B: SUPERFLUID DENSITY

The superfluid density can be understood as the stiffness of the system responding to the phase twists. Then, from the response function of phase twists, the superfluid fraction can be obtained. We consider to impose a phase twist $\mathbf{Q} = Q_x\hat{e}_x + Q_y\hat{e}_y$, i.e., a supercurrent as $\psi_\sigma(\mathbf{r}) \to e^{i\mathbf{Q}\cdot\mathbf{r}}\psi_\sigma(\mathbf{r})$. This imposed phase gives the system a kinetic energy, which corresponds to the free-energy difference $\Delta F(\mathbf{Q}) = F(\mathbf{Q}) - F(0)$, where $F(\mathbf{Q})$ is the free energy within the phase variation, and $F(0)$ is the free energy without the phase variation. In the limit $\mathbf{Q} \to 0$, such variation of free energy is approximately determined by the extra kinetic energy resulting from the imposed supercurrent,

$$\Delta F(\mathbf{Q}) \approx \sum_{i,j=x,y} \frac{Q_i Q_j}{2} \lim_{Q_{i,j}\to 0} \frac{d^2F(\mathbf{Q})}{dQ_i dQ_j} \equiv \sum_{i,j} \frac{1}{2} n_s^{(i,j)} m v_s^{(i)} v_s^{(j)} S, \tag{B1}$$

where $\mathbf{v}_s = \hbar\mathbf{Q}/\mathbf{m}$ is the velocity of superfluid and S is the area of the 2D system. We, then, can define the ratio of the superfluid density over the total density $\bar{n} = N/S$ as

$$\frac{n_s^{(i,j)}}{\bar{n}} \equiv \frac{m}{N} \lim_{Q_{i,j}\to 0} \frac{d^2F(\mathbf{Q})}{dQ_i dQ_j}, \quad i, j = x, y. \tag{B2}$$

Due to the reflection symmetry of the Hamiltonian, when $i \neq j$, $n_s^{(i,j)}$ vanishes. We, thus, introduce $n_{x(y)} \equiv n_s^{[x(y),x(y)]}$ to denote superfluid fraction along the x and y directions, respectively. As shown in Fig. 6, there is a nonzero superfluid density, characterizing the supersolid nature of the ground state. Furthermore, we also find that there is a jump in the superfluid density when the transition from the superfluid to the supersolid occurs, indicating its first-order nature.

[1] E. P. Gross, Phys. Rev. **106**, 161 (1957).
[2] E. P. Gross, Ann. Phys. (NY) **4**, 57 (1958).
[3] A. J. Leggett, Phys. Rev. Lett. **25**, 1543 (1970).
[4] B. K. Clark and D. M. Ceperley, Phys. Rev. Lett. **96**, 105302 (2006).
[5] M. W. Ray and R. B. Hallock, Phys. Rev. Lett. **100**, 235301 (2008).
[6] M. Boninsegni, Phys. Rev. B **79**, 174203 (2009).
[7] S. Balibar, Nature (London) **464**, 176 (2010).
[8] E. Kim and M. H. W. Chan, Nature (London) **427**, 225 (2004).
[9] T. Leggett, Science **305**, 1921 (2004).
[10] N. Prokof'ev and B. Svistunov, Phys. Rev. Lett. **94**, 155302 (2005).
[11] M. Boninsegni and N. V. Prokof'ev, Rev. Mod. Phys. **84**, 759 (2012).
[12] S. Sasaki, R. Ishiguro, F. Caupin, H. J. Maris, and S. Balibar, Science **313**, 1098 (2006).
[13] E. Kim and M. H. W. Chan, Phys. Rev. Lett. **97**, 115302 (2006).
[14] L. Pollet, M. Boninsegni, A. B. Kuklov, N. V. Prokof'ev, B. V. Svistunov, and M. Troyer, Phys. Rev. Lett. **98**, 135301 (2007).
[15] N. Prokof'ev, Adv. Phys. **56**, 381 (2007).
[16] N. Henkel, R. Nath, and T. Pohl, Phys. Rev. Lett. **104**, 195302 (2010).
[17] F. Cinti, P. Jain, M. Boninsegni, A. Micheli, P. Zoller, and G. Pupillo, Phys. Rev. Lett. **105**, 135301 (2010).
[18] N. Henkel, F. Cinti, P. Jain, G. Pupillo, and T. Pohl, Phys. Rev. Lett. **108**, 265301 (2012).
[19] S. Wessel and M. Troyer, Phys. Rev. Lett. **95**, 127205 (2005).
[20] I. Danshita and C. A. R. Sá de Melo, Phys. Rev. Lett. **103**, 225301 (2009).
[21] O. Tieleman, A. Lazarides, and C. Morais Smith, Phys. Rev. A **83**, 013627 (2011).
[22] L. Tanzi, E. Lucioni, F. Famà, J. Catani, A. Fioretti, C. Gabbanini, R. N. Bisset, L. Santos, and G. Modugno, Phys. Rev. Lett. **122**, 130405 (2019).

[23] F. Böttcher, J.-N. Schmidt, M. Wenzel, J. Hertkorn, M. Guo, T. Langen, and T. Pfau, Phys. Rev. X **9**, 011051 (2019).
[24] L. Chomaz, D. Petter, P. Ilzhöfer, G. Natale, A. Trautmann, C. Politi, G. Durastante, R. M. W. van Bijnen, A. Patscheider, M. Sohmen *et al.*, Phys. Rev. X **9**, 021012 (2019).
[25] J. Léonard, A. Morales, P. Zupancic, T. Esslinger, and T. Donner, Nature (London) **543**, 87 (2017).
[26] J.-R. Li, J. Lee, W. Huang, S. Burchesky, B. Shteynas, F. c. Top, A. O. Jamison, and W. Ketterle, Nature (London) **543**, 91 (2017).
[27] V. Galitski and I. B. Spielman, Nature (London) **494**, 49 (2013).
[28] J. Dalibard, F. Gerbier, G. Juzeliūnas, and P. Öhberg, Rev. Mod. Phys. **83**, 1523 (2011).
[29] N. Goldman, G. Juzeliūnas, P. Öhberg, and I. B. Spielman, Rep. Prog. Phys. **77**, 126401 (2014).
[30] H. Zhai, Int. J. Mod. Phys. B **26**, 1230001 (2012).
[31] H. Zhai, Rep. Prog. Phys. **78**, 026001 (2015).
[32] X.-L. Chen, J. Wang, Y. Li, X.-J. Liu, and H. Hu, Phys. Rev. A **98**, 013614 (2018).
[33] K. Zhou and Z. Zhang, Phys. Rev. Lett. **108**, 025301 (2012).